

# High-Resolution Seismic Reflection Profiling of the Fenhe Fault in Taiyuan City<sup>1</sup>

You Huichuan, He Zhengqin, Ding Zhifeng, Wu Jianping and Wu Qingju

Institute of Geophysics, China Seismological Bureau, Beijing 100081, China

---

In this paper, we demonstrate the high-resolution seismic reflection data for a depth range of several hundred meters across the Fenhe fault in Taiyuan city, China. In combination with the relevant borehole logs, these data provide useful constraints on the accurate position, geometry and deformation rate of the fault, as well as the kinematics of recent fault motion. The high-resolution seismic reflection profiling revealed that the western branch of the Fenhe fault is a high angle, eastward dipping, oblique-normal fault, and cutting up to the lower part of the Quaternary system. It was revealed that the top breaking point of this fault is at a depth of ~ 70m below the ground surface. A borehole log across the Fenhe fault permitted us to infer that there are two high-angle, oppositely dipping, oblique-normal faults. The eastern branch lies beneath the eastern embankment of the Fenhe river, dipping to the west and cutting into the Holocene-late Pleistocene strata with a maximum vertical offset of ~ 8m. Another borehole log across the northern segment of the Fenhe fault indicates that the western branch of this fault has cut into the Holocene-late Pleistocene strata with a maximum vertical offset of ~ 6m. The above-mentioned data provide a minimum average Pleistocene-Holocene vertical slip rate of 0.06 ~ 0.08mm/a and a maximum average large-earthquake recurrence interval of 5.0 ~ 6.7ka for the Fenhe fault.

**Key words:** Taiyuan city; Fenhe fault; High-resolution seismic reflection profiling

---

## INTRODUCTION

A set of NNE-near NS-trending faults has developed in the Shanxi faulted basin zone. These faults have undergone the 1303 Hongdong  $M$  8.0 earthquake, the 1683 Yuanping  $M$  7.0 earthquake, the 1695 Linfen  $M$  7½ earthquake, and other earthquakes. Thus, these faults are the seismogenic structures for large earthquakes in this basin zone (Deng Qidong et al., 1985; Xu Xiwei, 1989). The Fenhe fault in Taiyuan city is one of them and mainly developed in the northern depression of the Taiyuan basin in the middle segment of the basin zone. It is distributed roughly along the Fenhe river

---

<sup>1</sup> Received in October 2002. This project was sponsored by the State Planning Commission; Institute of Geophysics, China Seismological Bureau. Contribution No. 03FE1006, Institute of Geophysics, CSB.

in a nearly NS direction through the Taiyuan urban districts. Is this fault different from or similar to the other faults along which large earthquakes have occurred? Is there a similar seismic risk on this fault? In seeking the answers, it is necessary to exactly understand the concrete position and spatial structure of the fault, its slip rate, and the dynamic process of the recent movement. However, the Fenhe fault is buried below the ground surface. We can't determine its exact location or its recent movement from surface geological-geomorphic data alone. It is necessary to use a sounding method to obtain the underground data, so as to understand the geometrical structure and the movement history of the fault.

High-resolution seismic reflection profiling was one of the effective and reliable sounding tools used to find the buried fault. The sounding often used a seismic reflection wave method to determine the depth of interfaces between strata and the seismic velocity structure of the strata. This was in accordance with the kinematic and dynamic characteristics of seismic reflection waves from the interfaces of different physical properties in crustal media. During recent years, the method has been widely used to effectively resolve some geological problems (Yang Wencai, 1993; Xiong Zhangqiang et al., 1994; Dolan et al., 1997; Hao Shujian et al., 2001). The seismic reflection wave method has a set of mature techniques for field data collection and laboratory data processing, which were described in detail in many monographs, textbooks, and papers (Wang Zhendong, 1988; Wang Qinghai et al., 1991; Yu Shoupeng, 1993; Qian Shaohu, 1993; Xiong Zhangqiang et al., 2002).

The Fenhe fault runs through the Taiyuan city center. If an earthquake rupture takes place on the fault, it would cause heavy damage. Thus, in this paper we will focus our study on the exact location of the fault and its dislocation. The sounding area is located on the western bank of the Fenhe river in Taiyuan city. In order to effectively control the strike of the fault, two sub-latitudinal seismic profiling lines were laid out between the western embankment of the Fenhe river east of Nantun village and the western water channel at 600 ~ 1200 m south of Changfeng west road. The result of high-resolution seismic reflection profiling of the shallow crustal part (several hundreds meters) is given in this paper and the basic characteristics of the Fenhe fault, such as its exact position, the movement nature and the age of the fault along the profiling lines, have also been determined. In combination with drill data, the geometrical structure, kinematic and dynamic behaviors of the Fenhe fault are preliminarily discussed.

## 1. A BRIEF OF THE FENHE FAULT AND THE PROFILING AREA

### 1.1. *Geomorphic Features in the Area*

Taiyuan city is located in the northern part of the Taiyuan basin in the middle part of the Shanxi Plateau. The Fenhe river runs from north to south through the city. Ten or more nearly WE-trending gullies on both its sides run into the river. In addition to the development of the loess platform and the alluvial-proluvial fan in the mountain front, tectonic subsidence made most area of the basin interior open and flat. Thus, the relief of the area is slowly tilted from the mountain front to the Fenhe river. The sounding area is located on the western bank of the Fenhe river, where the landform is flat.

### 1.2. *The Quaternary Deposits and Tectonic Features in the Area*

The Cambrian to the Jurassic systems are distributed in the periphery of the Taiyuan basin, but the younger and the Quaternary deposits are developed within the basin. The Neogene system in the northern depression reach 310 m in thickness and discontinuously cover the underlying strata. The system is mainly lacustrine deposits, consisting of clay and silt-fine-grained sand with sand-gravel layers. The Quaternary system has well developed and its thickness reaches 200 ~ 400 m. It is made up of grey-brown fluvial-lacustrine sediments (Bureau of Geology and Mineral Resources of Shanxi Province, 1989).

The margin of the northern segment of the Taiyuan basin is controlled by the faults in the Xishan

Mountain front and on the western border of Dongshan Mountain, formed a sub-longitudinal asymmetric graben deep in the west and shallow in the east. Two sets of faults have developed within the graben (Fig. 1); many sub-longitudinal faults have been arranged in parallel and are cut by two sub-latitudinal faults into three segments. The formers are normal dextral strike-slip faults and the latter are normal sinistral strike-slip faults (Deng Qidong et al., 1985; Xu Xiwei, 1989).

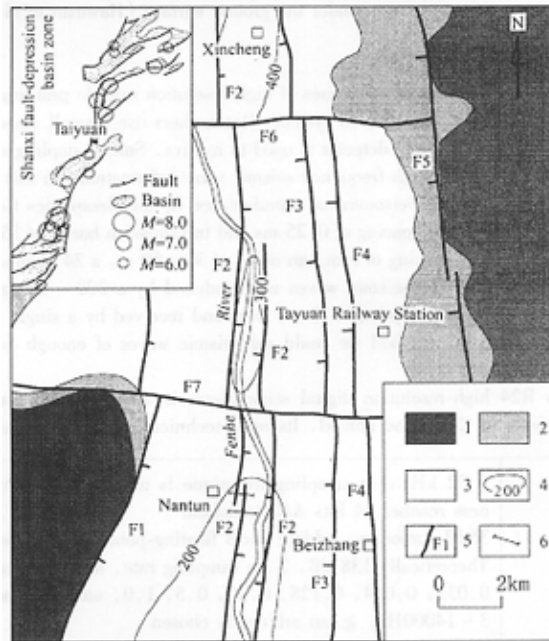


**Fig. 1**

Sketch of geological structure of the Taiyuan area

1. Mountain area; 2. Platform or proluvial fan; 3. Basin plain; 4. Quaternary subsidence center and thickness; 5. Fault and its number; 6. Location of sounding line; F1 - Xishan Mountain front fault; F2 - Fenhe fault; F3 - Qinxian fault; F4 - Beizhang fault; F5 - Dongshan fault; F6 - Sangei fault; F7 - Tianzhuang fault

### 1.3. A Brief of the Fenhe Fault

The Fenhe fault extends near the Fenhe river valley west of the central part of the basin in sub-longitudinal direction and then turns to a SWS direction south of the Taiyuan urban area. It consists of several 7 ~ 25 km long, high-angle, normal strike-slip faults in *en echelon* form (Xu Xiwei, 1989). In the studied area, this fault consists of both eastern and western branches and has been cut by WE-trending faults into three segments: the western branch of the northern segment is well developed and dips to the east, It controls a second-order Quaternary subsidence center. The middle segment consists of two branches dipping oppositely and controls a secondary Quaternary subsidence center in the Fenhe river valley. The southern segment is mainly the eastern branch dipping to the west and is developed on the eastern side of the Quaternary subsidence center in the southern part of the depression.

## 2. HIGH-RESOLUTION SEISMIC REFLECTION PROFILING

A common-reflection point, multi-coverage observation system is usually used in the seismic reflection wave method. It is effective for suppressing interference waves and improving signal-noise ratio. The seismic wave method can visually reflect the fluctuation of stratigraphic interfaces and is fairly effective for the detection of buried faults under the ground surface (Hawman et al., 2000).

### 2.1. Data Collection

The key point of the method and techniques of high-resolution seismic profiling is to arrange short and small channel spacing of the observation system. Researchers use a small amount of charge to induce seismic waves. A high-frequency detector is used to receive. Small sampling spacing and a wide-band recorder are used to acquire high-frequency seismic wave information. In this sounding operation we used a Strata View R24 Digital Seismometer manufactured by the Geometrics Company in the USA for recording. We used a sampling spacing of 0.25 ms and transmission bands of 35 ~ 200 Hz. An observation system with a channel spacing of 5 m, an offset of 30 ~ 50 m, a 24 channel unilateral receiver, and 6 stacks was adopted. The seismic waves were induced by a 200 ~ 400 g ammonium nitrate charge set down in a borehole at a depth of 1.3 ~ 1.5 m and received by a single 100 Hz high-sensitivity vertical detector. With this method we could get seismic waves of enough energy and an wider band spectra.

The Strata View R24 high-resolution digital seismometer is a device used for data collection in many engineering projects in China and abroad. Its main technical specifications are as follows:

A/D transform	A 32 kHz over-sampling technique is used and the processing effectiveness reaches 24 bits A/D transform
Pre-amplifier gain	36dB stationary, adding 24dB floating-point amplification
Dynamic range	Theoretically 138 dB, 2 ms sampling rate, and measured 113 dB
Sampling spacing	0.032, 0.064, 0.128, 0.25, 0.5, 1.0, and 2.0 ms
Frequency band	3 ~ 14000Hz, $\geq$ an arbitrarily chosen

Active fault is defined as a fault, which has been active since the late Quaternary. Thus, the stratigraphic boundary between the late Pleistocene and middle Pleistocene deposits became a marked interface for determining the existence of the active fault, while the base interface of the Quaternary system became an important object for the study of fault geometry and fault activity. In the design of the observation system, the detection depth for an optimal observation window was supposed to be 40 ~ 300 m. The related parameters were determined finally in a test of collected data and an examination of interference waves.

### 2.2. Data Processing

The high-resolution seismic reflection profiles used in geological interpretation were obtained by processing data collected with single shots in the field. The data processing was performed by using the Winseis Program prepared by the Kansas Company in the USA. The processes included data format transforming, channel editing, static correction, numerical filtering, dynamic correction, velocity scanning, and horizontal stacking. After a digital processing the horizontally stacked time profiles were obtained (Figs. 2 and 3). Abscissa  $a$  is the CDP number and its coordinates are two-way reflection time (ms). Comparing the reflection wave groups in the time profiles, we can determine the structural forms of the reflection layer. The corresponding interpretation profile is obtained from the stacking velocity data after velocity analysis in combination with the geological data and the velocity measurement

result from the boreholes.

The shallow seismic velocity obtained in the velocity analysis of the seismic reflection data has a larger error due to the short arrangement and small spacing of the channels in the high-resolution seismic reflection profiling. For this reason, in order to determine the seismic velocity in the late Quaternary deposits, the detection was performed in two boreholes. In combination with data from other neighboring holes we determined the velocity in the upper part of the Quaternary deposits ( $Q_{3,4}$ , the fluvial sediments) to be 1200 m/s and the velocity in the lower part ( $Q_{1,2}$ , fluvial sediments) to be 2240 m/s.

### 2.3. Time Profiles

#### 2.3.1. Seismic Reflection Interfaces

Two seismic reflection interfaces were determined in accordance with the correlation between reflection wave phases and the occurrence altitude and levels of the stratigraphic units. They are called the upper and lower reflection interfaces (Fig. 2 and Fig. 3). In fact, there are also an other 1 ~ 2 reflection interfaces existing faintly in the deeper part. They are not distinctive due to the insufficient energy for inducing the seismic wave.

*The upper reflection interface.* It consists of 2 ~ 3 strong phases with a high video-frequency in nearly horizontal occurrence and can be continuously traced. The two-way travel time is 85 ~ 110 ms. The features of the reflection wave above and below the interface are clearly different. The reflection wave energy above the interface is weaker and often displays a blank zone, sometimes a changing occurrence. The reflection wave energy below the interface is stronger, but its layering is sparse and nearly horizontally.

*The lower reflection interface.* It consists of 2 ~ 3 continuous strong phases in a nearly horizontal occurrence, with high video-frequency. The two-way travel time is 180 ~ 200 ms. The features of the reflection wave above and below the interface are clearly different. The reflection wave energy above the interface is weaker and sometimes displays a blank zone with relatively sparse layering. The reflection wave energy below the interface is slightly stronger and its layers are denser.

*The reflection interfaces in the deeper part.* 1 ~ 2 reflection interfaces can be faintly found along the sounding line No. 2. Most of them consist of one relatively strong phase with higher video-frequency, in a nearly horizontal occurrence. Most of them also extend intermittently.

#### 2.3.2. Seismic Reflection Layers

The geological media are separated by the upper and lower reflection interfaces into three (the upper, middle, and lower) sets of seismic reflection layers depending on the reflection wave features, velocity in the layers, for example.

*The upper set of reflection layers.* It occurs between the ground surface and the upper reflection interface. Its reflection wave energy is weaker and often displays a blank zone. Its occurrence sometimes varies. The two-way travel time changes less in its western part and more in the eastern part. The velocity in the layers is 1200 m/s.

*The middle set of reflection layers.* It occurs between the upper and lower reflection interfaces. Its reflection wave energy is not strong and sometimes displays a blank zone. Its layering is relatively sparse, but two-way travel time changes less. The velocity in the layers is 2240 m/s.

*The lower set of reflection layers.* The top of this set is the lower reflection interface. Its reflection wave energy is slightly strong and its layering is also denser. The velocity in this set is 2950 m/s.

*The age of the sets of seismic reflection layers.* Geological and drill data indicate that the Quaternary deposits are well developed with about 200 m thickness. The underlying deposits are the Neogene

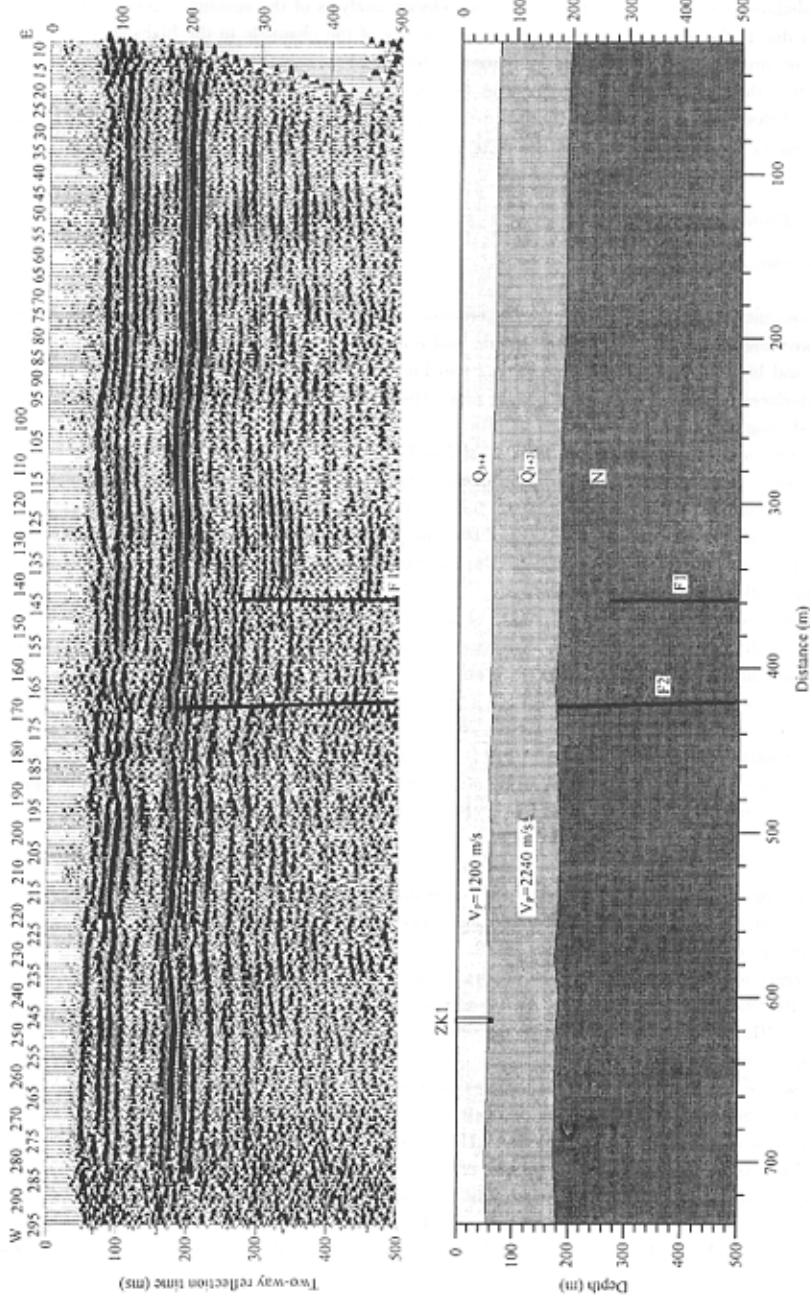


**Fig. 2** Seismic reflection profile of the No. 1 traverse across the Fenhe fault in Taiyuan city

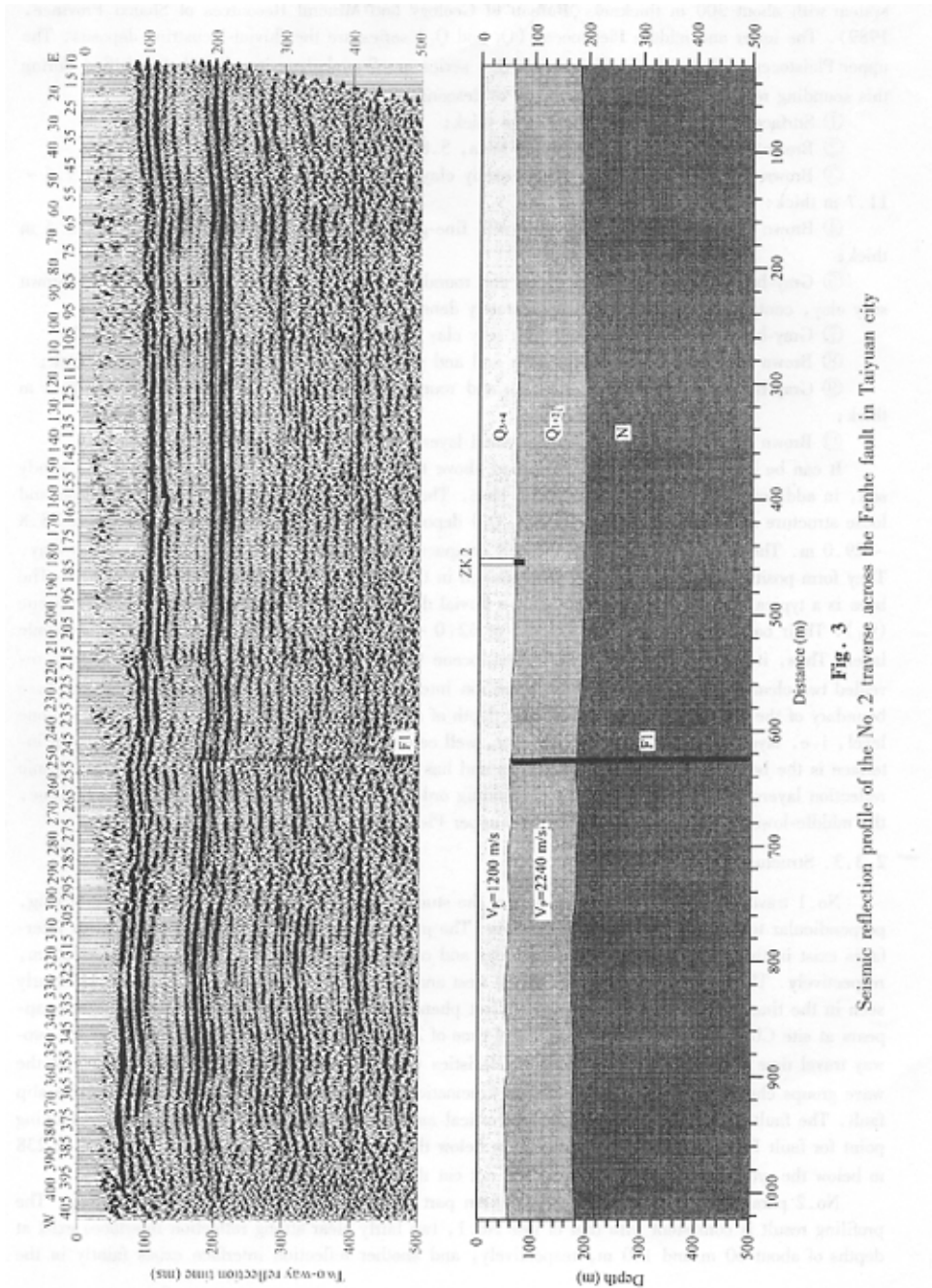


**Fig. 3** Seismic reflection profile of the No. 2 traverse across the Fenhe fault in Taiyuan city

system with about 300 m thickness (Bureau of Geology and Mineral Resources of Shanxi Province, 1989). The lower and middle Pleistocene ( $Q_1$  and  $Q_2$ ) series are the fluvial-lacustrine deposits. The upper Pleistocene ( $Q_3$ ) and the Holocene ( $Q_4$ ) series are fluvial deposits. Two holes drilled during this sounding revealed the strata, which are in descending order as follows:

- ① Surface cultivated soil, 0.5 ~ 1.0 m thick;
- ② Brown-yellow silty clay, containing mica, 5.8 ~ 7.5 m thick;
- ③ Brown and gray-brown fine-grained sandy clay, with powdered soil and small gravel, 9.5 ~ 11.7 m thick;
- ④ Brown and brown-yellow silty clay with fine-grained sand, containing mica, 9.5 ~ 10.5 m thick;
- ⑤ Gray-brown gravel with sand filling and rounded gravel, 0.8 ~ 1.0 m thick; ⑥ Gray-brown silty clay, containing mica fragments, moderately dense, 9.5 ~ 10.2 m thick;
- ⑦ Gray-brown and brown gravel, with silty clay, moderately dense, 10.0 ~ 19.5 m thick;
- ⑧ Brown silty clay, locally with sandy soil and gravel, containing mica, 2.0 ~ 5.0 m thick;
- ⑨ Gray-brown gravel with sand filling and rounded gravel, moderately dense.  $7.0 \geq 8.5$  m thick;
- ⑩ Brown silty clay, with fine-grained sand layer, compacted, unexposed.

It can be known from the data described above that the layers ① ~ ⑤ are mainly brown sandy soil, in addition to thin gravel layer at the base. They are of fine-grained material composition and loose structure and should be the Holocene ( $Q_4$ ) deposits. The base boundary lies at a depth of 28.8 ~ 29.0 m. The layers ⑥ ~ ⑨ are moderately compacted gray-brown sand-gravel layers and silty clay. They form positive rhythmic deposits, fine-grained in the upper part and coarse in the lower part. The base is a typical "basal gravel" layer, being a fluvial deposit. They were formed in the late Pleistocene ( $Q_3$ ). Their base boundary lies at a depth of 62.0 ~ 67.5 m. Layer ⑩ is a compacted rhythmic layer. Thus, it was formed in the middle Pleistocene ( $Q_2$ ). Therefore, the two sounding profiles revealed two clear and continuous seismic reflection interfaces: the upper interface represents the base boundary of the late Pleistocene deposits at a depth of about 60 m (the difference between them is one level, i. e. layer ⑨), a thin basal gravel layer, well cemented, with higher velocity) and the lower interface is the bottom of the Quaternary system and has a depth of about 200 m. The 3 sets of seismic reflection layers separated by them, in descending order, represents the Holocene-upper Pleistocene, the middle-lower Pleistocene series, and the upper Pleistocene, respectively.

### 2.3.3. Structural Analysis

No.1 traverse lies in the northern part of the studied area. It is sub-latitudinal and 760 m long, perpendicular to the major structure in the area. The profiling result indicates that two very clear interfaces exist in the seismic reflection time profiles and occur at depths of 50 ~ 70 m and 180 ~ 200 m, respectively. They tend to be shallower in the west and deeper in the east (Fig. 2). It can be clearly seen in the time profiles that a remarkable offset phenomenon of cophase axis of reflection waves appears at site CDP143 below the two-way travel time of 280 ms ( $F_1$ ) and at site CDP169 below the two-way travel time of 245 ms ( $F_2$ ). The characteristics (frequency, amplitude and travel time) of the wave groups change significantly and display kinematic and dynamic behaviors typical of a strike-slip fault. The faults at the two sites are nearly vertical and dip slightly to the east. The upper breaking point for fault  $F_1$  is at a depth of about 270 m below the ground surface and that for fault  $F_2$  is at 238 m below the ground surface. Thus, they did not cut through the Quaternary system.

No.2 parallel to No.1, lies in the southern part of the profiling area and is 1040 m long. The profiling result is consistent with that of line No.1, two fairly clear strong reflection interfaces exist at depths of about 60 m and 180 m, respectively, and another reflection interface exists faintly in the



deeper part. The two strong reflection interfaces are shallower in the west and deeper in the east (Fig. 3). It is clearly seen at site CDP253 between the two-way travel time of 135 ms and 450 ms ( $F_1$ ) that the cophase axis of the reflection waves is clearly offset, with the offset amplitude gradually reducing from the deep to the shallow part. The upper breaking point cuts into the lower part of the Quaternary system ( $Q_{1,2}$ ) at depth of 70 m below the surface, near the base boundary of the upper Pleistocene series. The fault is nearly vertical, with a vertical offset less of than 10 m, and displays a movement nature with a mainly normal faulting component but mainly a strike-slip movement.

In summary, the two seismic reflection profiles across the Fenhe fault in Taiyuan city revealed that two clear and continuous strong reflection interfaces exist commonly under the ground surface in the studied area. The upper interface lies at a depth of 60 m, at the base of the upper Pleistocene series, and the lower interface is at a depth of about 200 m, at the base of the Quaternary system. As described above, the sounding area is controlled by a set of NNE-sub-longitudinal structures, which have undergone strong dextral strike-slip movement. Therefore, the breaking points found on profiling lines No.1 and 2 indicate generally that there are sub-longitudinal high-angle strike-slip faults in the right stepover, as shown in Fig. 1. They are the western branches of the Fenhe fault. One of them, fault  $F_1$ , is controlled by an eastern breaking point on sounding line No.1 and a breaking point on sounding line No.2. It has cut the middle-lower Pleistocene series and the underlying deposits and has been covered with the Holocene-upper Pleistocene sediments. It indicates that the fault was activated in the early Quaternary and ceased in the late Quaternary. Comparative analysis of the offset deposits along the sounding profiles and the features of the seismic wave groups on both sides of the fault permitted us to know that fault  $F_1$  is a strike-slip fault with a less tensile dip-slip component. Fault  $F_2$  is controlled only by a western breaking point on sounding line No.1. The other *en echelon* branch that we determined to be the western branch of the Fenhe fault is inferred from the geological data near the sounding area (Bureau of Geology and Mineral Resources of Shanxi Province, 1989). It is worthy to note that the amount of movement along the stepover part of the fault is less than that along the main body of the fault that did not cut the Quaternary system.

### 3. DISCUSSION AND CONCLUSIONS

#### 3.1. The Exact Location and Geometry of the Fenhe Fault

In the past, the Fenhe fault attracted little attention and was not widely understood, as there was a lack of detailed and direct data on the fault, little information had been obtained either through regional geological investigation of basin structures or through local geological prospecting. Therefore, the location of the fault was shown differently in the various geological maps and the spatial geometrical structure of the fault was inferred. The profiling result, in combination with previous geological data (Bureau of Geology and Mineral Resources of Shanxi Province, 1989) provides a significant understanding of the fault, though the profiling was performed only in the one area. Firstly, the Fenhe fault was considered to be a single fault consisting of many segments distributed along the eastern bank of the Fenhe river. The profiling result indicates that a high-angle east-dipping fault exists beneath the western bank of the Fenhe river and is the western branch of the Fenhe fault. This was found after analysis of the sounding data in combination with the drill data. Therefore, the Fenhe fault should consist of both its branches. The western branch lies between the western embankment of the Fenhe River and the western water channel (Figs.1 and 4). Secondly, two branches of the fault in the middle and southern sections of the sounding area dip oppositely and have formed a longitudinal narrow graben. This controlled the development of the Fenhe river and its valley position. The northern segment of the fault is only a branch. The available data indicates that it dips to the north, so it is the western branch of the fault. Thirdly, two branches of the Fenhe fault are small distance apart, dip op-

positely, and extend downward to a depth at which they should be combined into a single fault. Because the southern and northern segments of the fault dip in opposite directions, the fault may have some hinge character for the movement. The northern segment of the eastern branch and the southern segment of the western branch are inferred to be the subordinate faults in the shallower part and extend downward to a certain depth at which they merge into the main body of the fault.

### 3.2. Tectonic Activity along the Fenhe Fault

Tectonic activity along the Fenhe fault reflects evidently on its controlling effect on the Quaternary subsidence centers. The Xincheng, the Central urban district, and the Jinyuan subsidence centers in the Taiyuan depression are controlled by the Fenhe fault (Fig. 1). The Xincheng subsidence center is located on the eastern side of the fault. The Central urban district-Fenhe subsidence center is between the two branches of the Fenhe fault, and the Jinyuan subsidence center is distributed on the western side of the fault. It reflects not only the vertical movement on the Fenhe fault, but also the strong horizontal movement along it, i. e. the dextral strike-slip movement along the fault, which makes the subsidence centers distributed in an "S" form or a quadrant. The western branch of the northern segment and the eastern branch of southern segment are the main controlling faults and dip oppositely.

It can be seen in Fig. 4 that the western branch of the southern segment has offset the middle Pleistocene deposits and the vertical dislocation at the base of the deposits is about 5 m, but the late Pleistocene deposits have not been offset. It is consistent with the results of the seismic profiling, indicating that the branch was not active in the late Quaternary. The eastern branch has offset the late Pleistocene deposits and the vertical dislocation at the base is about 8 m, while the vertical dislocation of the base of the middle Pleistocene deposits reaches 10 m or larger. The Fenhe river runs between the two branches. Fig. 5 shows a borehole log across the northern segment of the Fenhe fault. The two boreholes are close to each other and the local geological and geomorphic conditions are similar. Therefore, analysis of the lithological characteristics and thickness variation of the deposits indicates that the fault had undergone a movement with a normal faulting component, but its vertical offset was not large, less than 6 m in the late Quaternary.

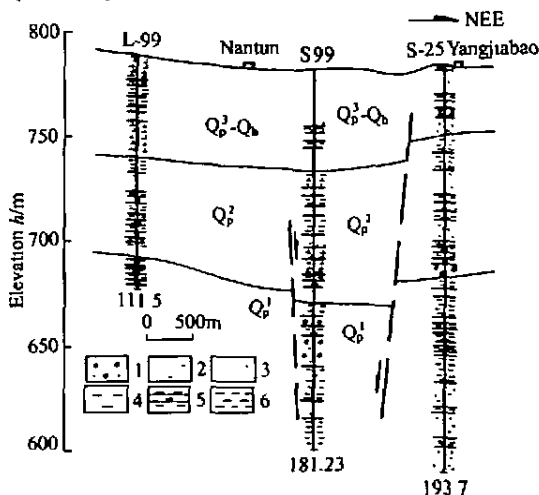


Fig. 4

Borehole log along Nantun-Yangjiapu profile across the Fenhe fault  
(revised after the Hydrogeological Team, Bureau of Geology and Mineral  
Resources of Shanxi Province, 1965)

1. Fine-grained gravel layer; 2. Gravel layer; 3. Sand layer;
4. Sandy soil layer; 5. Sandy clay layer; 6. Clay layer

### 3.3. Seismic Risk on the Fenhe Fault

The Fenhe fault is a late Pleistocene active fault. The seismic risk on the fault can be discussed from the following aspects:

(1) Slip rate. The Fenhe fault is a mainly dextral strike-slip fault. No horizontal movement indications were found, because the fault is located in the plain interior. Thus, its dextral strike-slip rate could not be determined. But drill data indicates that the vertical slip rate on the fault has been 6 ~ 8 m since the late Quaternary, which is slightly larger than that of fault No. 5 in the Tangshan area (about 5 m, Li Jianhua, 1998). If the time interval is taken to be 100 ka, the corresponding vertical slip rate will be 0.06 ~ 0.08 mm/a; If small earthquakes and non-seismic creep are not considered, the vertical dislocation caused by each large earthquake is assumed to be 0.4 m (the average vertical dislocation caused by the Tangshan earthquake), and the corresponding recurrence interval of large earthquakes will be 5.0 ~ 6.7 ka.

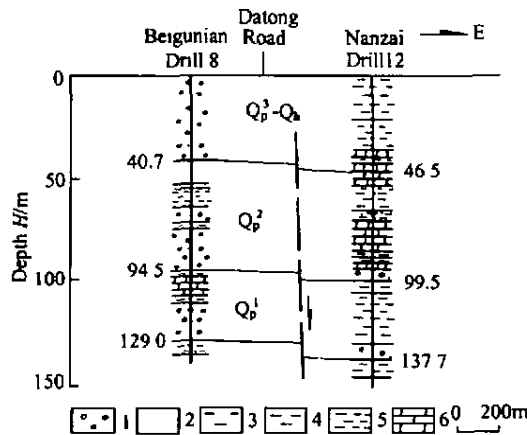


Fig. 5

Borehole log along Beigunian-Nanzai profile across the Fenhe fault (revised after the Institute of Geology, State Seismological Bureau, 1989)

1. Sand-gravel layer; 2. Silt-fine-grained sand layer; 3. Sandy soil layer;
4. Sandy clay layer; 5. Clay layer; 6. Gray-black sandy clay layer

(2) Basin structure. The geological characteristics of the northern depression of the Taiyuan basin are similar to those of the Linfen basin in the southern part and the Yuanping depression of the Xinding basin in the northern part of the Shanxi faulted basin zone. 1) Structurally they are the NNE-sub-longitudinal narrow-long shear basins and are connected with the ENE-NE-trending extensional basins, respectively. 2) They are controlled by the NNE-sub-longitudinal faults and have formed a mosaic graben. Their subsidence centers lies in the basin centers to the west and the thickness of the Quaternary deposits is in the range of 200 ~ 800 m. 3) The dips of the main controlling faults decrease from the central parts to the margins of the basins and the dip-slipping along the marginal faults is more remarkable, but striae with small angle in depression are often found, indicating a strong strike-slip movement along the faults (Research Group on Active Faults around Ordos Block, 1988). 4) These basins were formed in the early Pliocene and the sub-latitudinal transverse structures have developed in them. The structures underwent recent movement and had offset the major structures. 5) The extent of the structures and the strength of their movement are about equal to each other.

(3) The seismic activity and seismogenic structures. In all of history, no large earthquake has been recorded in the Taiyuan depression in which the Fenhe fault is located. Only some intermediate-

strong earthquakes of  $M \geq 5.0$  have occurred. But large earthquakes of  $M 8.0$  and  $M 7.0$  occurred in the Linfen basin and the Yuanping depression, which have similar tectonic structure, and where the seismogenic structures are NNE-sub-longitudinal normal strike-slip faults. Is the real difference in seismic risk on the faults or do other causes exist? We suggest that the seismic risk on the faults may be slightly different and not essentially distinct, because the basins and faults are much similar in qualitative and quantitative aspects. However, the difference is that in situ recurrence interval of large earthquakes is very long and the seismic activity is characterized by a variation of temporal-spatial sequence. Therefore, the seismic risk on the Fenhe fault exists objectively and enough attention must be paid to it.

## REFERENCES

- [1] Bureau of Geology and Mineral Resources of Shanxi Province. *Regional Geological Records of Shanxi Province*. Beijing: Geological Publishing House, 1989 (in Chinese).
- [2] Deng Qidong and You Huichuan. Structural characteristics and formation mechanism of fault-depression basin zones around Ordos Block, north central China. *Research on Recent Crustal Movement*, 1, Beijing: Seismological Press, 1985. 58 ~ 78 (in Chinese).
- [3] Dolan J F. High-resolution seismic reflection profiling of the Santa Monica fault zone, West Los Angeles, California. *Geophysical Research Letters*, 1997, 24 (16): 2051 ~ 2054.
- [4] Hao Shujian, You Feichuan. Precise shallow seismic sounding of Tangshan active fault. *Seismology and Geology*, 2001, 23 (1): 93 ~ 97 (in Chinese with English abstract).
- [5] Hawman R B, et al. Shallow seismic reflection profiling over Brevard zone, south Caroline. *Geophysics*, 2000, 65 (5): 1388 ~ 1401.
- [6] Li Jianhua, Hao Shujian, Hu Yutai, et al. Research on the activity of seismogenic fault for 1976 Tangshan earthquake. *Seismology and Geology*, 1998, 20 (1): 27 ~ 32 (in Chinese with English abstract).
- [7] Qian Shaohu. *Seismic Exploration*. Beijing: China University of Earth Sciences Press, 1993 (in Chinese).
- [8] Research Group on "Active Fault System around Ordos Block" of State Seismological Bureau. *Active Fault System around Ordos Block*. Beijing: Seismological Press, 1988. 89 ~ 113 (in Chinese).
- [9] Wang Qinghai and Xu Mingcai. *High-resolution Anti-interference Shallow Seismic Exploration*. Beijing: Geological Publishing House, 1991 (in Chinese).
- [10] Wang Zhendong. *Applied Technique of Shallow Seismic Exploration*. Peking: Geology Publishing House, 1988 (in Chinese).
- [11] Xiong Zhangqiang and Fang Genxian. Application of high-resolution seismic reflection to engineering prospecting of Xiamen Meijing Garden. *Bulletin of East China Geological Institute*, 1994, 17(3): 276 ~ 280 (in Chinese with English abstract).
- [12] Xiong Zhangqiang and Fang Genxian. *Shallow Seismic Exploration*. Beijing: Seismological Press, 2002 (in Chinese).
- [13] Xu Xiwei. *Characteristics of Neotectonics and Formation Mechanism of Shanxi Graben System*. Ph.D. Dissertation in Institute of Geology, State Seismological Bureau, 1989 (in Chinese with English abstract).
- [14] Yang Wencai. Application of computer-aided seismic topography to engineering exploration. *Geophysical and Geochemical Explorations*, 1993, 17(3): 182 ~ 192 (in Chinese).
- [15] Yu Shoupeng. *High-resolution Seismic Exploration*. Beijing: Oil Industry Publishing House, 1993 (in Chinese).

## About the Author

You Heichuan, born in 1959, graduated from the Department of Geomorphology and Quaternary Geology, Beijing(Peking) University, in 1982 and received his master's degree from the Institute of Geology, State Seismological Bureau in 1984. He is now an associate research professor at the Institute of Geophysics, China Seismological Bureau. He is engaged in active structures, the relationship between shallow and deep structures, and seismic safety evaluation.